https://doi.org/10.5194/egusphere-2026-719
Preprint. Discussion started: 16 February 2026

Community-scale metabolism of coral ecosystems persisting under marginal environmental conditions

Timothy B. King[1], Yu-De Pei[1], Joshua Bennett-Williams[1], Alex S.J. Wyatt[1]

[1]Department of Ocean Science, The Hong Kong University of Science and Technology, Clear Water Bay, Kowloon, Hong Kong

Correspondence to: Alex S.J. Wyatt (wyatt@ust.hk)

Abstract. Coral communities in Hong Kong persist under a range of natural and anthropogenic stressors, including strong seasonality, high bioerosion, sedimentation, and elevated nutrient levels. These challenging environmental conditions provide an opportunity to better understand how coral ecosystems may adapt to changing ocean conditions in the future. Here, we used in situ sensors to quantify high-resolution, community-scale net ecosystem production (NEP, organic carbon cycling) at three sites across a marine environmental gradient around Hong Kong. These communities were net respiring (negative NEP) across the gradient in both the wet (NEP_{mean}= -0.49 ± 4.83 mmol O_2 m^{-2} hr^{-1}) and dry seasons (NEP_{mean}= -0.21 ± 0.85 mmol O_2 m^{-2} hr^{-1}), with a significant increase in metabolic variability observed during the wet season (mean daily NEP range = 9.99 ± 13.34 mmo O_2 m^{-2} hr^{-1}) versus the dry season (2.38 ± 1.93 mmol O_2 m^{-2} hr^{-1}) . This study is the first to our knowledge to assess in-situ metabolic variability of coral communities persisting under marginal environmental conditions. Understanding natural community-scale variability is crucial for predicting how coral communities may adapt to changing ocean conditions, thereby providing vital insights into the future of globally threatened coral reef ecosystems.

1 Introduction

Coral ecosystems offer crucial ecosystem services, such as supporting biodiversity hotspots, providing storm protection for coastal communities and tourism-related income (Moberg & Folke, 1999). However, the future viability of these ecosystems is threatened by global stressors, including ocean warming (Hughes et al., 2017) and acidification (Doney et al., 2009), and local stressors such as pollution and sedimentation (Tuttle & Donahue 2022). We can better understand how coral communities might adapt and persist in the future by studying communities that are already surviving challenging and changeable environments. While accreting coral reefs generally thrive in shallow, clear waters, coral ecosystems can persist under extreme and marginal environmental conditions (Schoepf et al., 2023), albeit typically with lower coral species diversity, slower growth rates, and without appreciable carbonate accretion (Heery et al., 2018).

Coral community ‘extremeness’ can be generally defined as a deviation from optimum environmental conditions for coral growth, either in mean or variance, while coral community ‘marginality’ can be generally defined based on ecosystem functioning and community composition, with areas of low coral cover, diversity, or functioning being labelled as marginal

https://doi.org/10.5194/egusphere-2026-719
Preprint. Discussion started: 16 February 2026

(Schoepf et al. 2023). Coral reef functionality is often characterized by the flux and storage of energy and materials within the ecosystem (Bellwood et al., 2019). Extreme environments can still support vibrant coral communities that have high coral cover and diversity (Thomas et. al., 2018), but marginal conditions, by definition, limit functionality, as has been observed in the reduced coral diversity and growth forms around Hong Kong (Cybulski et al., 2020). Coral communities subject to extreme and/or marginal conditions span the globe (Burt et al., 2020) and understanding how they are currently responding to the challenges of global climate change can provide insights into how coral ecosystems might persist into the future. A key component of furthering understanding of how these corals are adapting to change is to understand how community metabolism, which reflects underlying ecosystem functionality, varies according to environmental constraints.

A lack of understanding of the close linkages between benthic metabolic processes and the chemistry of the overlying water column presents one of the major obstacles in accurately predicting how coral ecosystems will adapt to future changes in ocean conditions (Albright et al., 2013; Andersson & Gledhill, 2013). To address this, a benthic community's net ecosystem production (NEP) can be measured in-situ and tracked alongside any related changes in the overlying water column, since this process influences the chemistry of the surrounding seawater in predictable ways (Cyronak et al., 2018). NEP is proportional to the gradient in dissolved oxygen (DO; McGillis et al., 2011) and reflects the cycling of organic carbon and the balance between photosynthesis and respiration (Andersson & Gledhill, 2013).

The magnitude of NEP generated by the benthic community can change over space and time depending on the local biogeochemical (Page et al., 2019) and physical environment (Falter et al., 2012; Long et al., 2013). NEP will raise DO and pH through photosynthesis and lower DO and pH through respiration (Turk et al., 2015; Lowe et al., 2019). Additionally, NEP will naturally fluctuate over diel to seasonal timescales and can be linked to the diversity of benthic communities (Takeshita et al., 2018), with more diverse and rich ecosystems displaying greater metabolic variability (Page et al., 2017). This variability has not been assessed in-situ in a marginal coral environment like Hong Kong, which is subjected to chronic local stressors.

Coral communities in the waters around Hong Kong persist under both marginal and extreme environmental conditions due to natural climatology, and anthropogenic forcing (Goodkin et al., 2011; Duprey et al., 2017). Hong Kong's sub-tropical, monsoonal climate varies markedly throughout the year. The wet season, which lasts from April to October, is marked by higher water temperatures (up to 31 °C), higher nutrient and sediment loads into coastal waters, more rainfall, and decreased salinity due to increased freshwater flux. The dry season, which lasts from November to March, is distinguished by low water temperatures (down to 14 °C), little rain, and higher salinities (Morton, 1989). Other local stressors, such as bioerosion (Dumont et al., 2013; Yeung et al., 2021), recreational activities (Chung et al., 2013), and elevated eutrophication rates (Duprey et al., 2016), fluctuate spatiotemporally around Hong Kong and can have short- and long-term impacts on the health of coral communities. An east-west environmental-urbanization gradient linked to human populations and discharge from the Pearl River disproportionally affects Hong Kong's western waters. Therefore, most of Hong Kong's corals are now found farther away from the Pearl River Estuary, in the eastern, more oceanic waters of the territory (Duprey et al., 2020). In addition to this spatial gradient in coral distribution, temporal shifts in coral growth have been linked to seasonal fluctuations

https://doi.org/10.5194/egusphere-2026-719
Preprint. Discussion started: 16 February 2026

in water temperature, causing increased heat stress and coral bleaching during the summer and lower coral productivity and growth rates in the cooler winter months (McIlroy et al., 2019).

Turbid marginal environments have the potential to serve as refugia for functional coral communities due in part to high turbidity levels protecting the corals from heat and light stress, although they may be more susceptible to adjacent anthropogenic activities (Morgan et al., 2017, Sully & Van Woesik, 2020). Hong Kong coral communities may thus serve as a proxy for understanding how corals currently living in favorable habitats may adapt to changes that lead to more marginal conditions in the future, influencing their persistence and ongoing survival in the face of a range of natural and anthropogenically enhanced stressors.

Globally, community-scale metabolic rates over coral habitats remain under-examined (Platz et al., 2022). In Hong Kong, measurements of coral metabolism have only been made at the level of individual corals (Dellisanti et al., 2020), with no assessments of metabolic rates at community levels. Community metabolism can change rapidly across small spatial scales, and the results of individual coral-scale metabolic rates may not be adequate for extrapolation to the community as a whole (Page et al., 2017). Understanding community-level natural variability is thus crucial for assessing how coral communities may adapt to changing ocean conditions. Therefore, rather than extrapolating estimates from a single species, investigations should include the metabolic signal of the whole community (Edmunds et al., 2016) to better forecast how community functionality may change in the future (Kekuewa et al., 2021).

The main objectives of the study were to (1) characterize the natural spatiotemporal variability in coral community metabolism through in-situ NEP measurements along the environmental-urbanization gradient in Hong Kong, and (2) identify environmental factors that are the primary drivers of changes in coral community metabolic function. Such information on the natural variability and environmental drivers of coral community metabolism is essential to understand how coral health and community functionality will adjust to shifting local and global ocean conditions, including increasing prevalence of marginality.

2 Materials and methods

2.1 Study sites

Three study sites were selected to represent a spectrum of environmental conditions around Hong Kong that still support corals, from east to west: Tung Ping Chau (22.5451°N, 114.4326°E), Sharp Island (22.3639°N, 114.2903°E), and Sham Wan (22.1861°N, 114.1359°E) (Fig. 1).

https://doi.org/10.5194/egusphere-2026-719
Preprint. Discussion started: 16 February 2026

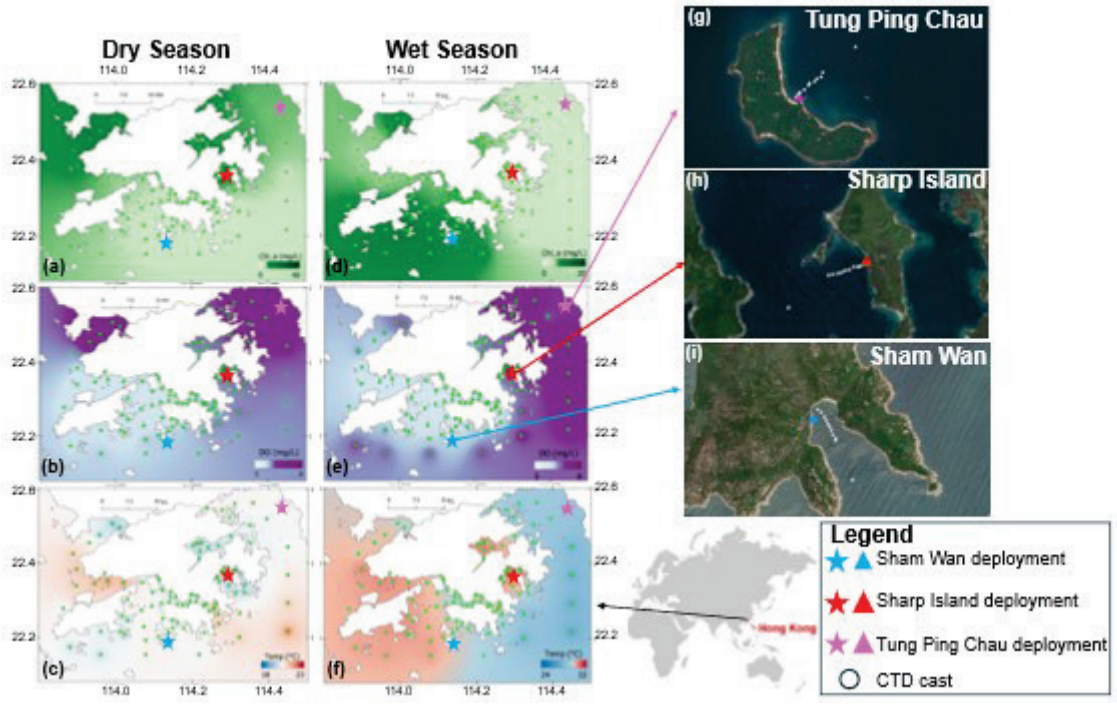

Figure 1. Marine environmental gradients and deployment locations around Hong Kong. Gradients during the dry (a, b, c; December 2021-January 2022) and wet (d, e, f; September-October 2022) season are shown for chlorophyll-a (a, 0-41 mg/L; d, 0-20 mg/L), temperature (b, 18-23 °C; e, 24-32 °C) and dissolved oxygen (c & f, 5-8mg/L) based on Environmental Protection Department (EPD) data measured at the sampling stations shown with green dots. Gradient flux instrument deployments (see Table 1) were undertaken to characterize community metabolism at 3 sites: (g) Tung Ping Chau (purple star), (h) Sharp Island (green star), and (i) Sham Wan (blue star). At each site, CTD casts were undertaken along a transect denoted by the white circles. Satellite images in g-i derived from (Imagery © 2023 NASA, Map data © 2023 Google). The inset map shows the location of Hong Kong (indicated by a red square) in relation to mainland China and the northern South China Sea.

Coral ecosystems in eastern Hong Kong have high species diversity and abundance and are comparatively unaffected by Pearl River discharge (Goodkin et al., 2011). Tung Ping Chau is especially isolated from the rest of Hong Kong, lying 10 km from the Hong Kong coast in Mirs Bay. While the waters surrounding Tung Ping Chau have previously been reported to have among the highest coverage and diversity of hard corals in Hong Kong (Xie et al. 2020), our surveys showed less coral cover around our deployment at Tung Ping Chau than at Sharp Island. However, Sharp Island in the past has shown evidence of higher bleaching rates than other sites in Hong Kong (Xie et al., 2020). During our deployments, outside peak summer conditions, there were no signs of significant bleaching affecting the community, likely due to rapid recovery of corals that bleached in August 2022, leading to near full recovery within months (Chung et al., 2024). The south of Hong Kong lies in the transitional zone where coral assemblages are still sporadically present, but abundances are limited by the impact of the

https://doi.org/10.5194/egusphere-2026-719
Preprint. Discussion started: 16 February 2026

Pearl River discharge (Duprey et al., 2016). Sham Wan, which is located in the middle of this transition zone, was selected to represent some of the more marginal conditions under which coral communities persist in Hong Kong.

The location of instrument deployments within sites were chosen based on visual inspection of the benthos by SCUBA divers such that the deployments were surrounded by relatively uniform coral communities on all sides that were roughly representative of the broader sites' composition. A summary of deployment parameters is available in Table 1. Changes in flow direction will lead to metabolism data being generated from different areas of benthic communities. Therefore, in this study, we selected deployment sites that were well surrounded, on all sides, by coral cover as uniformly high as possible to account for unpredictable flow patterns.

Table 1. Summary of deployments during the dry (2021) and wet (2022) seasons showing the location, season, deployment dates, the mean and range in depth of deployment (in m), deployment duration (in days), and mean (± S.E.) NEP value for each deployment.

Season	*Location*	*Dates*	*Depth (m)*	*Duration (days)*	NEP_{MEAN} *(mmol O_2 m^{-2} hr^{-1})*
Dry	*Sham Wan*	*23–30 Dec 2021*	*5.8 (4.7-6.7)*	*7*	*-0.37 ± 1.3*
	Sharp Island	*19–26 Nov 2021*	*3.3 (2.4-4.3)*	*7*	*0.12 ± 1.3*
	Tung Ping Chau	*30 Nov – 7 Dec 2021*	*3.8 (2.7-5.2)*	*8*	*-0.22 ± 0.9*
Wet	*Sham Wan*	*28 Oct – 11 Nov 2022*	*5.7 (4.5-6.8)*	*14*	*-0.37 ± 0.6*
	Sharp Island (May)	*18–24 May 2022*	*3.7 (2.7-4.9)*	*6*	*-1.39 ± 3.0*
	Sharp Island (Oct)	*29 Sept – 6 Oct 2022*	*3.6 (2.7-4.6)*	*7*	*0.15 ± 9.4*
	Tung Ping Chau	*11–21 Oct 2022*	*2.8 (2.0-3.6)*	*11*	*-0.59 ± 2.3*

To encompass major seasonal variations, deployments were carried out at each site during the dry season (Nov-Dec 2021) and at the end of the prolonged wet season in 2022 (October 2022; Table 1). An additional deployment was completed

https://doi.org/10.5194/egusphere-2026-719
Preprint. Discussion started: 16 February 2026

earlier in the wet season (May 2022) at Sharp Island. Hong Kong experienced its hottest Autumn on record (September-November) during 2022, with a mean air temperature of 26.4 °C (Hong Kong Observatory, 2022). Although October typically marks the transition to the dry season, prolonged elevated temperatures resulted in conditions more characteristic of the wet season extending later into the year than usual.

2.2 Water quality data and climatic conditions of Hong Kong

The environmental gradient around Hong Kong was characterized using periodic monitoring data collected by the Environmental Protection Department (EPD, https://cd.epic.epd.gov.hk/EPICRIVER/marine/?lang=en, date accessed Dec 15, 2023), focusing on the monthly data from the wet (September, October 2022) and dry season (December 2021, January 2022), closest to our deployment dates (Figure 1a-f). Surface-water data collected at 1 m depth was used because it best reflects the environmental conditions experienced by local coral communities due to their typically shallow distribution (1-6 m, Goodkin et al., 2011). For monitoring sites with multiple days of observations during the period of interest, values were averaged to give one seasonal value per station. The variables examined included dissolved oxygen (DO), turbidity, chlorophyll-a (chl-a), temperature, and salinity. These parameters were selected due to their ecological relevance to coral reef metabolic processes and availability across both seasonal periods.

2.3 Benthic community composition

The benthic community composition of these locations, including substrate composition and the cover for each coral genus, was characterized based on underwater video surveys conducted at each site from September–October 2020. The surveys used a GoPro Hero4 Black camera to capture video transects based on a timed (5 min) swim from a roving diver, moving in a spiral motion outward and away from the deployed gradient flux system. Benthic analysis was undertaken using CoralNet (Beijbom et al., 2015). Photo quadrats were extracted from each video transect at approximately 10 second intervals. Due to poor quality (i.e., too blurry) of a few extracted images, we eventually were only able to obtain 28, 28, and 25 usable photo quadrats for Tung Ping Chau, Sharp Island, and Sham Wan, respectively. From each extracted photo quadrat, 100 random points were overlaid on each image with an annotation area set to exclude 20 % of the area from the peripheral to ensure no overlap between images. Major biotic and abiotic benthic groups (sand, rock, rubble) were annotated, and hard corals were identified to a finer genus level with notes on their health status (i.e., live and dead) when possible. Artificial items and unidentifiable or unknown objects were labelled as “Others-Abiotic” and “Unknown/Unidentifiable”, respectively. Benthic community composition was presented as percent cover (%) for each benthic category. Macroalgae and turf algae were included as groups as well, but no significant coverage was identified for record at any of our sites. This finding is supported by past benthic studies completed in Hong Kong that showed algal abundance peaking during early Spring months and decreased substantially during the summer and early winter months (Yeung et al., 2021; Cheung Wong et al., 2022).

https://doi.org/10.5194/egusphere-2026-719
Preprint. Discussion started: 16 February 2026

2.4 Coral community metabolism measurement: gradient flux approach

To characterize the metabolic rates of Hong Kong coral communities, we collected autonomous measurements of benthic metabolism at high temporal frequencies (minutes) using a gradient flux (GF) approach, which tracks chemical and velocity gradients in the benthic boundary layer to estimate benthic metabolic rates (McGillis et al., 2011). The gradient flux technique has been used to assess NEP (McGillis et al., 2011; Turk et al., 2015; Takeshita et al., 2016; Coogan et al., 2018) on natural coral reefs, and at coral restoration sites (Platz et al., 2020). The GF approach relies on estimates of the mean chemical flux of DO from the benthic boundary layer to calculate NEP. In this study, the GF instrumentation consisted of two DO sensors (MiniDOT, Precision Measurement Engineering (PME), Vista, California, USA) and two velocimeters (Vector, Nortek, Norway) positioned at two heights above the benthos, Z_1 and Z_2. The lower height (Z_2) was positioned 8cm above the substrate, and the top height (Z_1) was 124cm above the substrate. The two DO sensors (accuracy = ±9.5 µmol kg^{-1}) were cross calibrated immediately after each deployment to correct for any offset between the two sensors that could impact the DO gradient and to minimize the impact of the uncertainty associated with the sensor accuracy. Fluxes of DO (mmol m^{-2} h^{-1}) were calculated using Eq. (1) (McGillis et al., 2011; Platz et al., 2020):

$$J_{DO} = \rho u^{*} \kappa \left(\frac{DO_{z1} - DO_{z2}}{ln\left(\frac{z_1}{z_2}\right)} \right) \quad (1)$$

where ρ is the seawater density (kg m^{-3}), u^* is the friction velocity (m s^{-1}), κ is the Kármán constant (0.40). This value is widely used for turbulent boundary layers and is supported by observations from coastal and reef environments, where κ typically falls within 0.35–0.50 (e.g., Gross & Nowell 1983). Although κ can vary with local roughness and wave–current interactions, its inclusion in the diffusivity term is linear; therefore, using κ = 0.40 is appropriate and provides a robust estimate for our sites. As above, Z_1 and Z_2 are the higher and lower pump heights (m), respectively. DO_{zx} is the chemical concentrations (µmol kg^{-1}) at the respective heights z_x (z_1 or z_2). The friction velocity was calculated using Eq. (2) as described in McGillis et al. (2011):

$$u^{*} = \kappa \left(\frac{U_{z1} - U_{z2}}{ln\left(\frac{z1}{z2}\right)} \right) \quad (2)$$

where U_z is the 3-axis water velocity at the respective sensor height (m s^{-1}).

Metabolic rates are proportional to these chemical fluxes (McGillis et al., 2011) and were calculated based on Eq. (3) as:

$$NEP = -(J_{DO}) \quad (3)$$

2.5 High frequency in-situ characterization of prevailing environmental conditions

The salinity (S) of the seawater was determined using a miniature CTD sensor (DEFI-CT, JFE Advantech, Tokyo, Japan) attached halfway between the two sensor heights on the GF frame. At each height, the respective velocimeter was used to

https://doi.org/10.5194/egusphere-2026-719
Preprint. Discussion started: 16 February 2026

measure, in addition to water velocity, the pressure (P) and temperature (T) of the seawater. During each deployment, a photosynthetically active radiation (PAR) sensor (MiniPAR, PME, Vista, California, USA) was also deployed directly on the benthos next to the gradient flux system to record incident light levels, far enough away to avoid shading by the instrument. All sensors collected data every 60 seconds and were averaged over 10 minutes for final data analysis.

We also measured the vertical structure of the water column, in terms of T (°C), S (ppt), DO (mol L^{-1}), and chl *a* (mg L^{-1}), along an onshore-offshore transect across each coral community using a RINKO-profiler CTD (ASTD102, JFE Advantech, Tokyo, Japan). Due to logistical constraints, casts were only performed during the wet season deployments. Ten casts were made per site with the exact location of each cast shown by the white dots in Fig 1g-i.

2.6 Data analyses

All calculations related to metabolism were performed in MATLAB (R2020b, The MathWorks Inc, Natick, Massachusetts, USA).

2.6.1 Data pre-treatment

Metabolic estimates were omitted when the top sensor velocity was lower than the bottom sensor velocity, showing that there was no law-of-the-wall relationship between the substrate boundary layer and the overlying water column (Platz et al. 2020). Additionally, data was not used for further analysis when the bottom velocity was too low ($<10^{th}$ percentile) to meet the prerequisites for the presence of a turbulent boundary layer.

A non-steady state boundary layer unsuitable for gradient flux analysis was indicated when the standard deviation of the 60-second DO measurements within each 10-minute averaged time period was in the top 10% of the distribution ($> 90^{th}$ percentile), determined for each deployment individually; data was discarded in such cases. ADV vector velocities were omitted when the correlation of any individual beam was < 50 %. If > 10 % of the burst sample (more than 1 of the 10 samples in each burst) was omitted, then that burst sample was not included in the 10-minute average velocity values used for further analysis, similar to the filter methods used in Coogan et al. (2022).

The 10-minute average values were used to provide time series for all environmental variables. Approximately 54.47 % of the dry season data and 62.94 % of the wet season data was removed with these filters applied, averaged for all deployments, omitting for Sham Wan in the wet season, where 86.04 % of data was removed largely due to a malfunction with the bottom DO making metabolism calculations impossible. Hourly-averaged NEP rates were used for plotting these time series. Any gaps in the time series are the result of either sensor failure due to water leakage or battery malfunction or, in the case of measurements of metabolism, violations of the conditions required for gradient flux calculations described above.

2.6.2 Statistical analyses

To assess spatial and diel variation in community metabolism, we conducted non-parametric statistical tests on NEP for each deployment. Analyses were performed separately for the dry season and wet season datasets. Timestamps were categorized

https://doi.org/10.5194/egusphere-2026-719
Preprint. Discussion started: 16 February 2026

into "Day" (7am-6pm) and "Night" (6pm-7am). Mean values were computed separately for each time category at each site. To test for significant differences in NEP between Day and Night, we applied the Mann–Whitney U test for each site individually. A Bonferroni correction was used to adjust for multiple pairwise comparisons ($\alpha = 0.05$). For deployments with valid data in both diel periods, the Mann–Whitney U statistic, raw p-value, and Bonferroni-adjusted p-value were calculated.

To identify the environmental variables most strongly associated with changes in NEP during each deployment, we quantified pairwise correlations between NEP and measured environmental parameters. Prior to this analysis, NEP values were regressed against PAR to isolate the light-driven component of NEP variability that would otherwise obscure the relationship between PAR and other measured variables (Khrizman et al., 2025). For each deployment, a simple linear model of the form:

$$NEP_{expected} = \alpha \times PAR + C \quad (4)$$

where α is the photosynthetic efficiency coefficient determined through the slope of the NEP/PAR relationship, and C is the intercept at zero irradiance. The residuals of this model,

$$NEP_{residual} = NEP_{observed} - NEP_{expected} \quad (5)$$

represent the portion of NEP variability independent of irradiance. Pearson correlation coefficients (r) and associated p-values were then computed between both the original NEP and the light-removed NEP residuals and each environmental predictor variable (water velocity, temperature, depth and salinity). Only relationships that were statistically significant ($p < 0.05$) were retained for result reporting and discussion.

Because assumptions of normality and equal variance were not met for several variables in the extracted EPD dataset, we employed the Mann-Whitney U test to determine whether median values of each parameter differed significantly between seasons. A significance threshold of $p < 0.05$ was used to identify meaningful seasonal differences. Simple linear regression was used to determine the correlation between PAR measured in-situ and global solar radiation derived from HKO weather data to examine light attenuation at the benthos. Global solar radiation was converted from Mj m^{-2} hr^{-1} to PAR units of µmol m^{-2} s^{-1} for slope comparison using a two-step process. First, global solar radiation values were converted to irradiance in watts per square meter (W m^{-2}) by multiplying by 277.78, recognizing that 1 MJ m^{-2} h^{-1} equals 277.78 W m^{-2}. Subsequently, to approximate PAR, the irradiance values were multiplied by an empirical conversion factor of 2.02 µmol J^{-1}. This factor reflects the proportion of solar energy within the PAR spectrum (400–700 nm) and is consistent with values reported in previous studies (Wang et al., 2024). The complete conversion formula is as follows:

$$PAR = Global\ solar\ radiation\ x\ 561.1 \quad (6)$$

Data from the HKO was analyzed according to a targeted dataset corresponding to the instrument deployment periods in the dry season (November–March 2021) and wet season (April–October 2022). For each environmental variable, we parsed and combined all relevant stations that measured a variable of interest (Light: Sai Kung; Wind speed; Sai Kung, Ping Chau and Lamma Island; Rainfall: Sai Kung, Ping Chau and Lamma Island). Values were grouped into wet season (April–October)

https://doi.org/10.5194/egusphere-2026-719
Preprint. Discussion started: 16 February 2026

and dry season (November–March) for the long-term dataset. For the deployment-time-specific dataset, seasonal grouping followed calendar year (i.e., dry = 2021; wet = 2022). We calculated seasonal means, standard deviations (±SD), and ranges for each variable. To test significant differences between wet and dry seasons within each dataset, we first assessed the normality of the data using the Shapiro-Wilk test. All variables were found to deviate significantly from a normal distribution ($p < 0.05$), so non-parametric Mann-Whitney U tests were used to compare medians between seasons. Kruskal-Wallis and associated post-hoc Dunn's test was used to test for difference in weather variables between deployments within seasons as well.

3 Results

3.1 Environmental conditions

3.1.1 Characterization of the vertical biophysical profile across sites

CTD casts measuring temperature, DO, and chl *a* were completed in October 2022 to assess the vertical water column structure at each site (Fig 2). Temperature along the Tung Ping Chau transect was spatially uniform (Fig 2b), averaging 28.0 ± 0.1 °C (range = 27.9–28.3 °C) with minimal vertical stratification ($\Delta T = T_{surface} - T_{bottom} = 0.18$ °C). Dissolved oxygen concentrations were similarly homogeneous (5.69 ± 0.13 mg L^{-1}; range = 5.48–5.94 mg L^{-1}) with only $\Delta DO = 0.18$ mg L^{-1} difference between surface and bottom layers (Fig 2c). Chlorophyll concentrations were low to moderate (0.79 ± 0.28 µg L^{-1}; range = 0.35–1.42 µg L^{-1}) and exhibited weak vertical gradients (Fig 2a), indicating well-mixed, oxygenated conditions across the CTD transect. The narrow temperature and DO ranges observed in the contour plots support limited water-column stratification and low variability with distance from shore. Sharp Island displayed the greatest vertical and spatial variability among the three sites. Temperatures averaged 29.2 ± 0.4 °C (range = 28.7–29.8 °C) (Fig 2e) with a mean surface–bottom gradient of 0.8 °C, reflecting moderate thermal stratification. Dissolved oxygen varied substantially (Fig 2f), ranging from 2.27 to 5.99 mg L^{-1} (mean 5.53 ± 1.1 mg L^{-1}), with a large surface–bottom difference ($\Delta DO = 2.6$ mg L^{-1}). The DO contour plot shows an oxygen minimum near the seabed in offshore casts. Chlorophyll concentrations (mean 0.79 ± 0.67 µg L^{-1}; range = 0.22–2.99 µg L^{-1}) (Fig 2d) increased offshore and at depth, aligning with enhanced stratification and possible subsurface productivity layers. Overall, the sharper vertical gradients at Sharp Island indicate stronger water column stability and low DO conditions in deeper water compared to the other sites.

At Sham Wan, temperature averaged 25.3 ± 0.9 °C (range = 24.0–26.8 °C) (Fig 2h) with modest vertical gradients ($\Delta T \approx 0.24$ °C). Dissolved oxygen was slightly higher on average than at the other sites (6.04 ± 0.5 mg L^{-1}; range = 5.90–7.69 mg L^{-1}) (Fig 2i) and showed weak stratification ($\Delta DO = 0.47$ mg L^{-1}). Chlorophyll concentrations were lower and more uniform (0.67 ± 0.37 µg L^{-1}; range = 0.06–1.48 µg L^{-1}) (Fig 2g), consistent with vertically mixed, well-flushed conditions within this semi-exposed embayment. The CTD transects highlight limited vertical structure and relatively high oxygenation throughout the water column, suggesting efficient turbulent exchange and minimal stratification.

https://doi.org/10.5194/egusphere-2026-719
Preprint. Discussion started: 16 February 2026

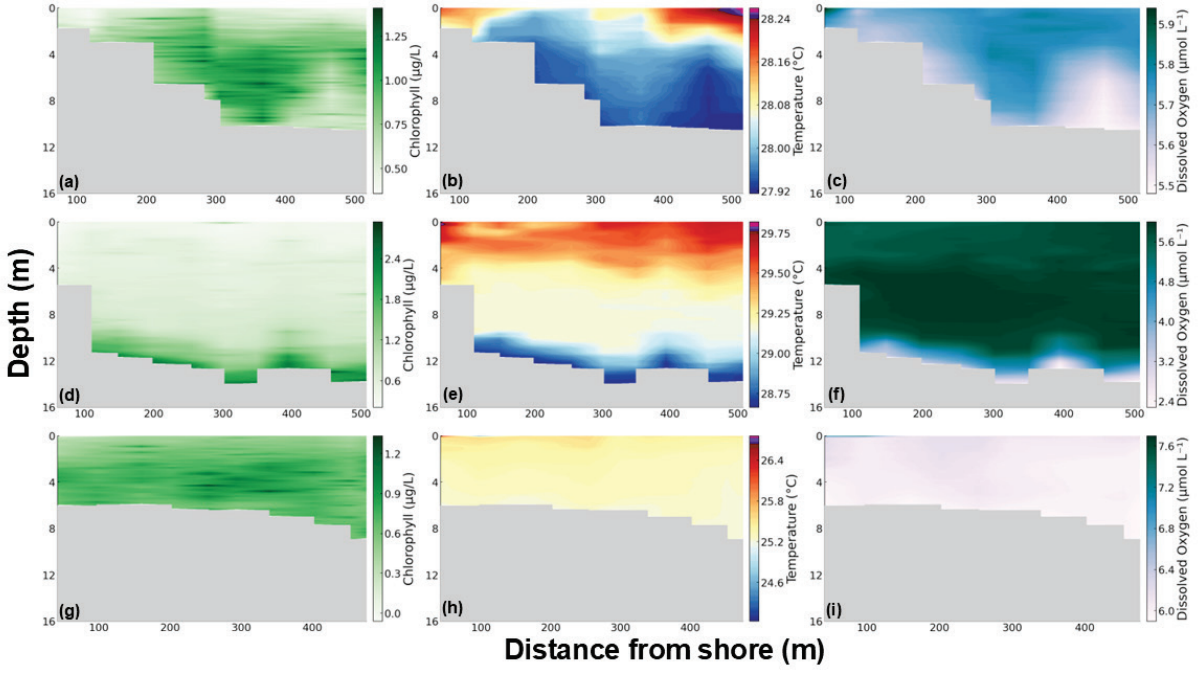

Figure 2. Vertical water column structure at each site. Contours show (A, D, G) chl a (in mg/L), (B, E, H) temperature (in °C) and (C, F, I) dissolved oxygen (in mg/L) based on CTD casts taken in October 2022 at each of the deployment sites. Tung Ping Chau (row 1): (A) chl a, (B) temperature and (C) DO. Sharp Island (row 2): (D) chl a, (E) temperature and (F) DO. Sham Wan (row 3) (G) chl a, (H) temperature, and (I) DO. The distance from shore of the CTD casts is shown on the x axis.

3.1.2 Seasonality in the environmental water quality gradient

Based on EPD data collected during both deployment seasons, the wet season was less saline, more turbid, and displayed higher temperatures and lower DO than the dry season. Mann-Whitney U-tests revealed significant differences in the means between seasons of each variable tested (p-value <0.05), except for chl-a, which was not significant (p-value = 0.079; Table S 1). The wet season (Figure 1d, e, f) exhibited highly variable turbidity, ranging from 0.9 to 384.2 NTU, with a mean value (± standard deviation) of 27.9 (±56.4). Chl-a ranged from 0.2 to 18 µg L^{-1}, with a mean value of 3.2 (±3.5). Salinity in the dry season ranged from 17.5 to 33.9 psu, with a mean value of 31.1 (±2.5). DO ranged from 3.0 to 7.5 mg L^{-1}, with a mean value of 5.4 (±0.8). Temperatures in the wet season ranged from 24.6 to 31.2 degrees Celsius, with a mean value of 28.4 (±1.4).

The dry season (Figure 1a, b, c) displayed less turbid, more saline water, lower temperatures, and higher DO compared to the wet season, with only marginal difference seen between seasons in chl *a* levels. Dry season turbidity ranged from 5.2 to 183.9 NTU, with a mean value of 19.3 (±28.1). Chl a values ranged from 0.2 to 41 µg L^{-1}, with a mean value of 2.9 (± 4.8). Salinity values ranged from 18.8 to 34.4 psu, with a dry season mean value of 33.2 (±1.8). Dissolved oxygen ranged from 4.3

https://doi.org/10.5194/egusphere-2026-719
Preprint. Discussion started: 16 February 2026

to 10.1 mg L^{-1}, with a mean value of 6.4 (±0.8). Temperature values ranged from 17.6 to 22.5 degrees, with a mean value of 20.2 (±1.1).

3.1.3 Atmospheric weather conditions

During the deployment periods, weather data similarly showed significant differences between wet and dry seasons for solar radiation and wind speed. Solar radiation was higher in the wet season (1.02 ± 1.05 MJ m^{-2} h^{-1}) than in the dry season (0.86 ± 0.91 MJ m^{-2} h^{-1}; $U = 2.31 \times 10^5$, $p = 0.0052$). Wind speed was significantly greater during the wet season (4.10 ± 2.67 $m \cdot s^{-1}$) compared to the dry season (3.02 ± 2.10 m s^{-1}; $U = 6.69 \times 10^5$, $p < 0.0001$). However, rainfall did not differ significantly between seasons during the deployment periods (wet: 0.11 ± 0.93 mm h^{-1}; dry: 0.02 ± 0.16 mm h^{-1}; $U = 5.04 \times 10^5$, $p = 0.696$). Weather data was also significantly different between deployment times within seasons as well. In the dry season, global solar radiation, wind speed, and rainfall were all significantly different between the Tung Ping Chau and Sham Wan deployment (Table S2). Dry-season Sharp Island deployment had significantly different wind speed and rainfall compared to Tung Ping Chau and Sham Wan, respectively. During the wet season, Tung Ping Chau and Sham Wan deployments had significantly different global solar radiation and rainfall. Additionally, Sharp Island's wind speed differed from Tung Ping Chau, and the rainfall differed compared to during the Sham Wan deployment (Table S2).

3.1.4 In-situ environmental conditions

Environmental conditions differed significantly between seasons when averaged across all sites. The wet season (Figure 3g-l) had higher average daytime PAR (194.21 ± 100.23 µmol s^{-1}) and average water temperature (25.89 ±2.13 °C) compared to the dry season (55.53 ± 34.81 µmol s^{-1}, 21.88 ±1.27 °C) (Figure 3a-f). Dissolved oxygen and salinity were lower in the wet season (181.76 ±27.35, 32.77 ±0.59 ppt) compared to the dry season (202.25 ±14.62, 33.72 ± 0.27). The direction of the dominant water flow remained constant from dry to wet season at all three sites. (Figure S1). Sharp Island displayed the most extreme values for many of the environmental variables recorded; in the wet season it had the highest mean water temperature (28 °C), lowest mean DO (165 µmol kg^{-1}), and lowest salinity (32.1 ppt), indicating more extreme conditions at the site over and above seasonal variations. Mean values and ranges for all environmental variables measured at each site and season can be found in Supplementary Information (Table S3, Table S4).

https://doi.org/10.5194/egusphere-2026-719
Preprint. Discussion started: 16 February 2026

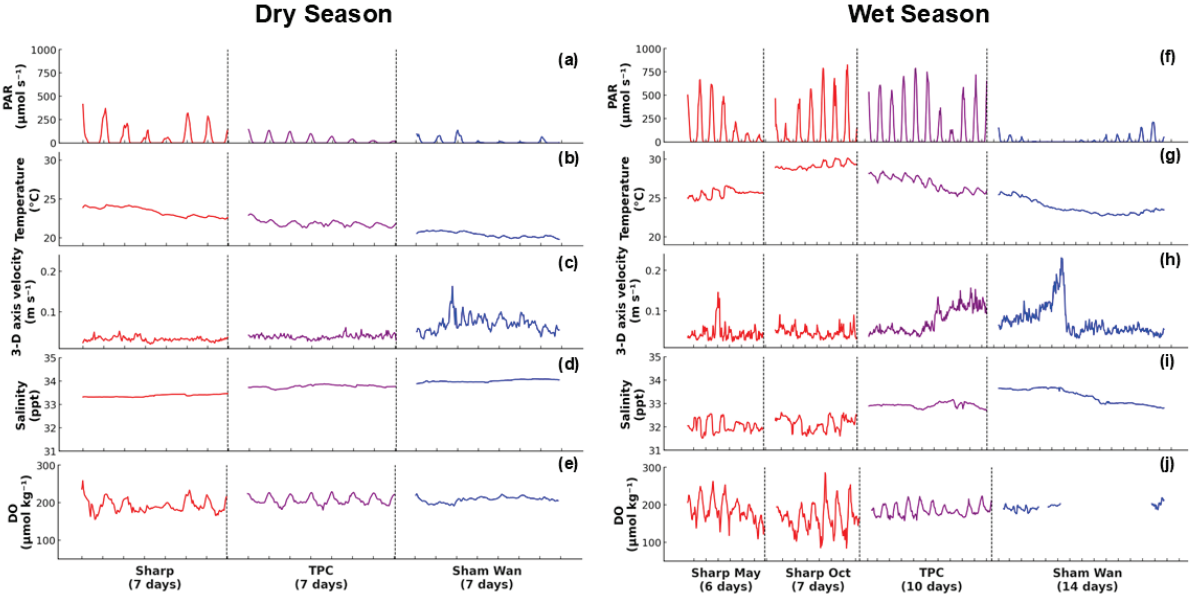

Figure 3. Comparison of prevailing environmental conditions measured during each deployment in the (a-e) dry and (f-j) wet seasons. Panels show PAR (µmol s^{-2}; a, f), temperature (°C; b, g), water velocity (m s^{-1}; c, h), salinity (ppt; d, i), and dissolved oxygen (µmol kg^{-1}; e, j) for Tung Ping Chau (blue lines), Sharp Island (black lines) and Sham Wan (red).

3.1.5 Benthic community composition

The estimated benthic community compositions are shown in Table 2. Focusing on major components of the benthic substrate (> 1 %), Tung Ping Chau was dominated by rock/rubble (38.89 ± 24.34%), live coral (36.14 ± 29.59 %), sand (21.14 ± 16.75 %), and dead coral (4.36 ± 7.71 %). The dominant coral genera present (reported as percent of total benthic cover) were *Porites* (2.89 ± 6.75 %), *Acropora* (8.04 ± 17.52 %), and *Platygyra* (23.86 ± 21.26 %). At Sharp Island, the substrate was predominately composed of live coral (65.75 ± 22.84%), with sand (18.14 ± 14.01 %), rock/rubble (10.71 ± 8.26%), and dead coral (3.66 ± 4.05 %). Within the live coral cover, *Acropora* (46.46 ± 25.99 %), *Pavona* (17.32 ± 21.25 %) and *Porites* (1.36 ± 3.08%) dominated the site. At Sham Wan, the benthos was mainly rock/rubble (59.4 ± 24.82 %) and sand (36.6 ± 26.16%), with only a small amount of live coral (3.84 ± 7.37 %). The only coral species observed in any numbers here was *Plesiastrea* (2.72 ± 7.37 %) supporting the selection of the site as a control due to its very low coral cover and sandy and rocky substrates.

https://doi.org/10.5194/egusphere-2026-719
Preprint. Discussion started: 16 February 2026

Table 2. Benthic community composition around the deployment locations at Tung Ping Chau, Sharp Island and Sham Wan as percentage total benthic cover. Tung Ping Chau's live coral cover was dominated by Platygyra sp. while Sharp Island was dominated by Acropora sp. Corals were largely absent from Sham Wan, which was dominated by rock/rubble/dead coral and sand.

	Acropora (%)	Pavona (%)	Porites (%)	Platygyra (%)	Plesiastrea (%)	Sand (%)	Rock/Rubble/Dead Coral (%)	Live Coral (%)	Dead coral (%)
Tung Ping Chau	8.04 ± 17.52	0.00 ± 1.50	2.89 ± 6.75	23.86 ± 21.26	0.00 ± 0.00	21.14 ± 16.75	38.89 ± 24.34	36.14 ± 29.59	4.36 ± 7.71
Sharp Island	46.46 ± 25.99	17.32 ± 21.25	1.36 ± 3.08	0.00 ± 2.60	0.00 ± 0.00	18.14 ± 14.01	10.71 ± 8.26	65.75 ± 22.84	3.66 ± 4.05
Sham Wan	0.00 ± 0.00	0.00 ± 0.00	0.00 ± 0.00	0.00 ± 0.00	2.72 ± 7.37	36.60 ± 26.16	59.40 ± 24.82	3.84 ± 7.37	0.00 ± 0.00

3.2 Benthic community metabolic rates

3.2.1 Dry season

Significant spatial and diel variability in NEP was detected during the dry season (Figure S2), with Tung Ping Chau and Sham Wan displaying net respiration (negative NEP) and Sharp Island NEP being slightly net productive. Diel comparisons of NEP within each site revealed significant differences between day and night (Figure 4a-c). Mann–Whitney U tests yielded statistically significant contrasts at Sharp Island ($p < 0.001$, daytime NEP = 0.31 ±1.47 $mmolO_2\ m^{-2}\ hr^{-1}$, nighttime NEP = -0.31 ±0.44 $mmolO_2\ m^{-2}\ hr^{-1}$) and Tung Ping Chau ($p < 0.001$, daytime NEP = 0.15 ±0.87 $mmolO_2\ m^{-2}\ hr^{-1}$, nighttime NEP =-0.69 ±0.72 $mmolO_2\ m^{-2}\ hr^{-1}$), indicating a shift from net autotrophy to net heterotrophy over the diel cycle. Sham Wan did not show significant differences between day and night NEP ($p = 0.176$, daytime NEP = -0.40 ±0.36 $mmolO_2\ m^{-2}\ hr^{-1}$, nighttime NEP = -0.34 ±0.30 $mmolO_2\ m^{-2}\ hr^{-1}$).

https://doi.org/10.5194/egusphere-2026-719
Preprint. Discussion started: 16 February 2026

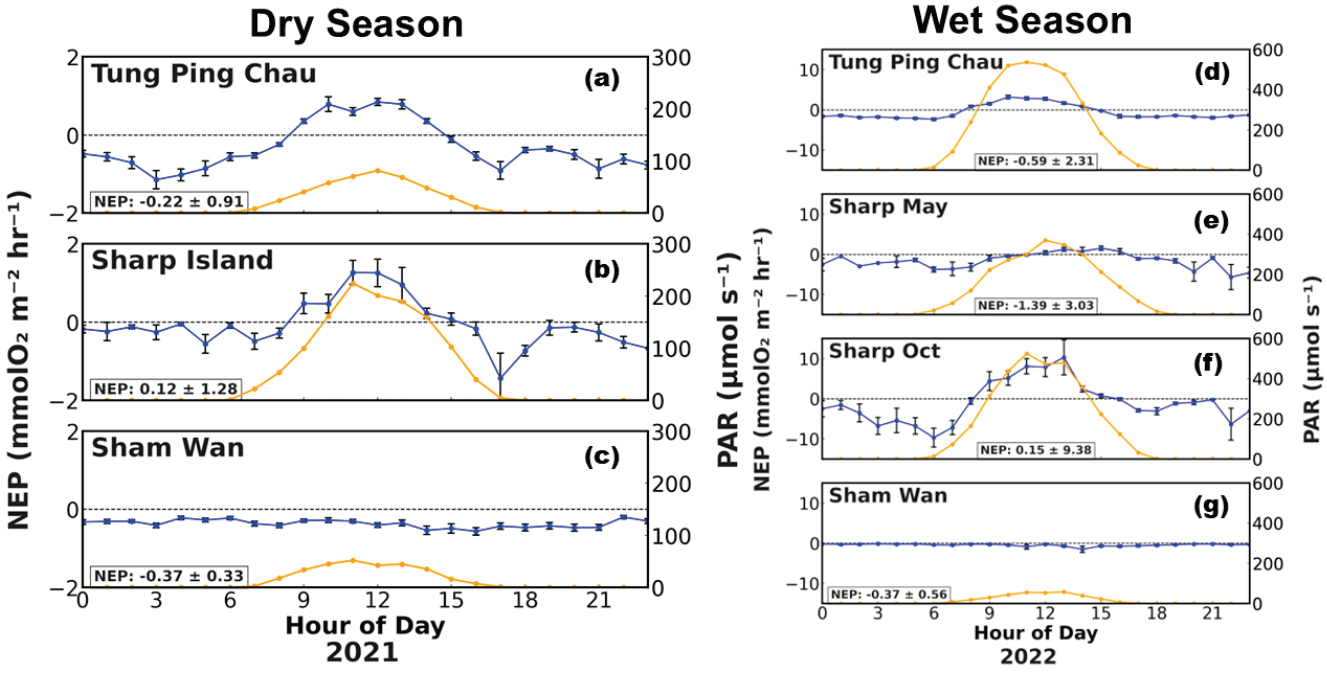

Figure 4. Diel composite plots of hourly averaged NEP (blue line) and PAR (orange line) for the dry season (a-c) and wet season (d-g) deployments. Error bars represent ± standard error of the mean NEP for each hourly bin. Text boxes show the mean ±SD NEP (mmolO_2 m^{-2} hr^{-1}). Note the expanded NEP and PAR axis ranges for the wet season figures relative to the dry season to capture the larger variability observed during the wet season.

3.2.2 Wet Season

In the wet season, all sites were net respiring (-NEP) except for Sharp Island in October which was slightly net productive. NEP also exhibited significant diel variation across all deployments (Figure S3). Mann–Whitney U tests revealed consistent and significant differences in NEP ($p < 0.001$) between day and night at all sites (Figure 4d-g). Tung Ping Chau NEP (daytime = 0.77 ±2.48 mmolO_2 m^{-2} hr^{-1}, nighttime = -1.78 ±1.28 mmolO_2 m^{-2} hr^{-1}) and Sharp Island NEP in both May (daytime = -0.63 ±2.85 mmolO_2 m^{-2} hr^{-1}, nighttime = -2.65mmolO_2 m^{-2} hr^{-1}) and October (daytime = 2.10 ±9.67 mmolO_2 m^{-2} hr^{-1}, nighttime = -1.78 ±1.28 mmolO_2 m^{-2} hr^{-1}) was significantly greater during the day than at night. Sham Wan NEP was significantly lower ($p = 0.0051$) during the day (-0.53 ±0.80 mmolO_2 m^{-2} hr^{-1}) versus the night (-0.27 ±0.28 mmolO_2 m^{-2} hr^{-1}).

3.3 Environmental drivers of NEP

3.3.1 Dry season

At Sharp Island, NEP (Figure S4**)** was strongly correlated with PAR ($r = 0.57$, $p < 0.001$), while weak negative correlations were also observed with bottom depth ($r = -0.16$, $p = 0.010$) and salinity ($r = -0.14$, $p = 0.026$). After removal of the PAR

https://doi.org/10.5194/egusphere-2026-719
Preprint. Discussion started: 16 February 2026

effect, none of these variables remained significantly correlated with the NEP residuals, indicating that NEP variability at this site was almost entirely governed by light availability.

At Tung Ping Chau, NEP also showed a significant positive correlation with PAR (r = 0.61, $p < 0.001$), while no other environmental parameters displayed significant relationships with either NEP or NEP residual. This suggests that community metabolism at Tung Ping Chau during the dry season was tightly coupled to irradiance and largely insensitive to variation in flow, temperature, or salinity.

In contrast, Sham Wan exhibited a broader range of significant relationships. NEP was positively correlated with bottom velocity ($r = 0.14$, $p = 0.002$), negatively correlated with bottom temperature ($r = -0.22$, $p < 0.001$), and positively correlated with salinity ($r = 0.12$, $p = 0.005$). These same variables remained significant after removing the PAR effect, with NEP residuals correlated with velocity ($r = 0.14$, $p = 0.001$), temperature ($r = -0.23$, $p < 0.001$), and salinity ($r = 0.13$, $p = 0.004$). This persistence of correlations in the light-removed dataset indicates that hydrodynamic and thermal processes exerted independent control on community metabolism at Sham Wan.

3.3.2 Wet season

At Sharp Island in May (Figure S5), NEP was significantly correlated with PAR (r = 0.53, p < 0.001) and water velocity ($r = 0.24$, $p < 0.001$). After removal of the PAR effect, NEP residuals remained significantly correlated with velocity ($r = 0.17$, $p = 0.014$), temperature ($r = 0.24$, $p < 0.001$), and salinity ($r = -0.16$, $p = 0.020$), indicating additional light-independent influences on benthic metabolism during this deployment.

In October at Sharp Island, NEP was strongly correlated with PAR ($r = 0.63$, $p < 0.001$), as well as temperature ($r = 0.32$, $p < 0.001$), depth ($r = -0.36$, $p < 0.001$), and salinity ($r = -0.11$, $p = 0.045$). However, none of these secondary correlations persisted in the NEP residuals, demonstrating that NEP variability was primarily driven by light and diurnally covarying thermal and hydrographic changes.

At Tung Ping Chau, NEP exhibited a very strong relationship with PAR (r = 0.72, p < 0.001) and a weaker positive correlation with velocity ($r = 0.09$, $p = 0.009$). These relationships disappeared for the NEP residuals, suggesting that short-term fluctuations in flow and temperature were largely covariant with light availability.

In contrast, Sham Wan 2022 showed significant correlations of NEP with PAR ($r = 0.41$, $p < 0.001$), bottom velocity ($r = 0.12$, $p = 0.006$), and bottom temperature ($r = -0.22$, $p < 0.001$). The NEP residuals remained significantly related to both velocity ($r = 0.11$, $p = 0.012$) and temperature ($r = -0.20$, $p < 0.001$).

4 Discussion

A growing number of studies have focused on community-scale metabolism over coral assemblages, utilizing primarily autonomous methods (Takeshita et al., 2018; Platz et al., 2022). To our knowledge, this is the first study assessing coral community metabolic rates in a marginal, highly urbanized environment. Quantifying how production rates naturally vary over

https://doi.org/10.5194/egusphere-2026-719
Preprint. Discussion started: 16 February 2026

space and time across the range of environmental conditions found around Hong Kong can help to better predict how corals may adapt to future ocean conditions amid ever-increasing rates of coastal urbanization and global change. To this end, interpretation of the spatiotemporal patterns in rates of NEP we have quantified over coral communities around Hong Kong will assist in identifying natural baseline variability in community metabolism and how such communities may adapt to future ocean conditions.

4.1 Spatiotemporal patterns in NEP

4.1.1 Seasonality in NEP

As might be expected for the challenging conditions coral communities face in Hong Kong, all our observations, across sites and seasons, indicated that these communities are net respiring or only slightly net productive, with average net respiration rates (-NEP) ranging from -1.39 ± 3.03 to 0.15 ± 9.38 mmol O_2 m^{-2} hr^{-1}. This suggests that the coral communities across Hong Kong are limited in their photosynthetic capacity, or that respiring organisms' metabolic rates exceeds rates of photosynthesis. PAR was shown to be a consistent primary driver of NEP rates during this study, so prolonged periods of cloudy weather could have a serious effect on suppressing NEP in this region. Hong Kong generally experiences reduced light conditions (4.0 kWh m^{-2} day^{-1}, Figure S6) (Hong Kong Observatory 2025) compared to other coral rich environments around the world, such as the Great Barrier Reef (5.0 - 6.0 kWh m^{-2} day^{-1}, SolCast Pty Ltd. 2025), the Caribbean (5.0 - 6.5 kWh m^{-2} day^{-1}, NASA Langley Research Center 2025), and the Red Sea (6.0 - 7.0 kWh m^{-2} day^{-1}, SolarGIS s.r.o. 2025). In combination with the strong net respiration signals seen during night hours in these coral communities (Mean NEP_{day} = 0.42 ± 4.21 (mmol O_2 m^{-2} hr^{-1} versus Mean NEP_{night} = -1.26 ± 2.39 mmol O_2 m^{-2} hr^{-1}), cloudy days and turbid water conditions will act in unison to suppress production rates in these communities. Despite the wet season displaying environmental conditions more conducive to positive NEP (higher PAR), these communities exhibit similar low production year-round, regardless of season. Past studies in Hong Kong have also documented that low light continues to limit productivity in these coral communities (McIlroy et al., 2019; Cybulski et al., 2020), along with limiting the distribution of coral assemblages (Yeung et al., 2021). This suggests that, unlike other reef communities where NEP is reduced during the winter, but elevated during summer (Falter et al., 2012; Stoltenberg et al., 2020), in Hong Kong it is negative year-round. This worrying trend may be enhanced in the future as an increase in cloud cover and a corresponding decrease in surface solar radiation have been observed in Hong Kong over the past decades (Hong Kong Observatory 2022). It must be noted that attempts to fit a photosynthesis–irradiance (PI) relationship to the observed NEP data were unsuccessful, as NEP did not approach saturation with increasing PAR at any site. The absence of a discernible P_{max} suggests that the ambient light regime in these Hong Kong coral communities remained below saturating levels for photosynthesis throughout the study period. This pattern is consistent with chronic light limitation, likely driven by high turbidity that has been shown to limit community productivity in other light-limited environments (Law et al., 2023).

More pronounced net respiration was evident in the wet season compared to the dry season, with negative NEP more than double during the wet (NEP_{mean}= -0.49 ± 4.83 mmol O_2 m^{-2} hr^{-1}) than dry (NEP_{mean}= -0.21 ± 0.85 mmol O_2 m^{-2} hr^{-1}). This

https://doi.org/10.5194/egusphere-2026-719
Preprint. Discussion started: 16 February 2026

suggests that seasonal changes in the wet season favor respiration processes over photosynthetic processes in the coral communities. Other factors that could have led to lower NEP in the wet season are lower salinity, pH, and DO in the wet season compared to the dry season (Table S3, Table S4), which could have led to increased physiological stress on the community as a whole and lessened their ability to maintain higher productivity (Cryer et al., 2023).

Weather patterns could also have had a role in changing community metabolic rates. Higher rainfall in the wet season, as measured at the HKO weather stations closest to the deployment sites, could also have contributed to the lower NEP values. Increased rainfall could lead to increased runoff, decreased salinity, increased organic matter input and subsequent organic matter respiration, and increased stratification of the water column due to freshwater intrusion (Goodkin et al., 2011; Zhou et al., 2012). Future studies should investigate in more detail, utilizing in-situ sensors with increased temporal resolution, what factors influence the relative level of both chemical and physical stratification in the water column to better elucidate the impact rainfall or other sources of runoff may have on strength of stratification.

Greater stratification in the water column will lead to the gradient flux measuring NEP values that are artefacts of a non-mixed water column, where an accumulation of the chemical concentration in the bottom layer due to less mixing will lead to a greater magnitude signal in NEP , but one that is not caused by the benthic metabolism. Thus, during periods of strong stratification, the gradient flux may not be an appropriate method to measure NEP (Coogan et al., 2022; Takeshita et al., 2016). The effect of the temperature gradient on NEP rates was monitored and assessed to account for this possible methodological artefact in our dataset. The strength of temperature stratification varied spatiotemporally between sites and seasons (Figure S7, Figure S8) but did not exceed > 0.5°C at any time during the deployment, therefore it was not considered to significantly affect the metabolism measurements of this study. However, we recommend future studies utilizing the gradient flux technique in strongly stratified waters to measure the salinity at both the top and bottom depth to better account for the influence of stratification on metabolism measurements. The gradient flux method also cannot be used during periods of intense water column mixing due to the lack of a steady state boundary layer and the deterioration of a present law-of-the-wall relationship in the velocity profile with respect to the substrate. An illustration of this in our dataset was during the wet season Tung Ping Chau deployment, on Oct 17, Typhoon Nesat impacted Hong Kong coastal waters, causing intense water mixing. Following this storm event, until the end of the deployment time (Oct 18-21), NEP rates could not be calculated due to the bottom water velocity (z_1 = 0.08cm) being consistently greater than the top velocity (z_2= 124cm), violating this assumption necessary for GF NEP calculations. Future studies should include analysis of weather conditions during deployment periods to reveal periods where intense stratification or water column mixing may be occurring, especially studies done during seasons with increased storm frequency such as the wet season in Hong Kong (Hong Kong Observatory, 2025).

4.1.2 Spatial patterns in NEP

Sham Wan displayed the lowest diurnal and seasonal variability and ranges in NEP during our study. The minimal diurnal variation in NEP likely reflects the relatively low metabolically active benthic diversity at the site (Figure 4) compared to the two other sites dominated by hard coral.

https://doi.org/10.5194/egusphere-2026-719
Preprint. Discussion started: 16 February 2026

Additionally, the deeper deployment depth, which reflected the lack of coral assemblages at shallower depths where a steep rocky wall borders the shore, likely contributed to reduced NEP due to lower light levels and lower water temperatures found in a couple of meters deeper water. The observations at Sham Wan highlights the likelihood that, as coral abundance and overall diversity decline westward across Hong Kong (Duprey et al., 2016, 2020; McIlroy et al, 2024), the metabolic activity of the benthic community likely decreases. Lower abundance communities, similar to Sham Wan, likely encapsulate the declines in coral community function expected with westward movement across Hong Kong as both water quality and diversity declines.

However, high diversity does not always equate to positive rates of productivity if other environmental variables act to dampen NEP. Despite being described as one of Hong Kong's most diverse coral communities, NEP values at Tung Ping Chau were net respiring. Nighttime respiration processes (Nighttime NEP_{mean} = -1.35 ± 1.90 (mmol O_2 m^{-2} hr^{-1}), in addition to daytime respiration, outweighed any daytime photosynthesis (Daytime NEP_{mean} = 0.46 ± 1.90 mmol O_2 m^{-2} hr^{-1}) occurring at this site. Coral bleaching was also recorded at Tung Ping Chau in July and August, due in large part to the warm temperatures seen during the summer of 2022 (Zhao et al., 2023). Bleached corals are expected to reduce NEP rates as photosynthetic algae are expelled from coral tissue during bleaching (Lombardi et al., 2000) but the coral animal remains alive and respiring, decreasing the ratio of photosynthesis to respiration (Schoepf et al., 2018). Additionally, if bleaching is sustained over long periods of time, coral mortality will increase, and communities will become more algal dominant (Haas et al., 2016).

While Tung Ping Chau exhibited consistently net-respiring conditions, possibly exacerbated by bleaching-related declines in photosynthesis, Sharp Island was the only site to display net productivity, doing so in both the dry season (NEP_{mean} = 0.12 ± 1.28 mmol O_2 m^{-2} hr^{-1}) and in October in the wet season (NEP_{mean} = 0.15 ± 9.38 mmol O_2 m^{-2} hr^{-1}). However, this site also showed significantly greater metabolic variability than the other two sites, with greater productivity signals during the day but also large respiration signals at night. During the wet season, nighttime oxygen depletion was so extreme that during certain hours, periods of moderate to severe hypoxia (61-92 µmol kg^{-1}) (Pezner et al., 2023), reaching levels as low as 70.98 µmol kg^{-1}, occurred, and persisted for up to several hours at a time (Figure S3b,c). This oxygen depletion at Sharp Island could be a result of upwelling of oxygen-depleted water from offshore, as was seen in the CTD cast conducted at Sharp Island, or from in-situ respiration processes occurring within the community. Regardless, hypoxic conditions measured in the benthic water at Sharp Island warrant further investigation as they are a cause for a concern for the coral at the site, with prolonged exposure to low oxygen conditions shown to have negative effects on coral health and function (Pezner et al., 2023).

4.1.3 Underlying causes of suppressed productivity in Hong Kong coral communities

Despite coral community compositions differing markedly, all sites were net respiring in both seasons. This suggests that, despite often forming major structural components of the habitat, corals themselves may be less dominant contributors to overall metabolism, with significant metabolic contributions potentially coming from other components of the community. Heterotrophic organisms that could influence the metabolic signals often found in abundance in Hong Kong's coral communities, such as sea cucumbers (Schneider et al., 2011), urchins (Yeung et al., 2021), oysters (Lau et al., 2020) and other

https://doi.org/10.5194/egusphere-2026-719
Preprint. Discussion started: 16 February 2026

cryptic taxa (McIlory et al., 2024). There is also evidence that corals persisting in turbid coastal water have adapted to their conditions through trophic plasticity that allows them to be more heterotrophic over time (Travaglione et al., 2023), offsetting losses due to sustained light limitation through feeding on abundant nutrient sources. The combination of a greater abundance of non-calcifying, respiring organisms and more heterotrophic corals may have led to the stronger net respiration seen in these marginal habitats. Future studies should make sure to account for variations in the abundance and composition of non-calcifying, respiring organisms when interpreting community metabolic rates, as they may dominate marginal environments such as Hong Kong.

Coral bleaching, unprecedented at the time, was recorded throughout the region, including Hong Kong, beginning in July 2022 (Zhao et al., 2023). While most corals were recorded as recovered by November 2022 (AFCD Reef Check 2022), it is unclear the extent of impact this bleaching event would have had on the corals' metabolism. However, it is known that bleaching severely damages coral communities' ability to maintain positive NEP by taking away a key source of photosynthesis. Increased respiration rates lead to environments of elevated pCO2 and decreased DO, which are conducive to net dissolution by hampering coral's ability to calcify (Comeau et al. 2014), increase sediment dissolution rates (Comeau et al., 2014), and increasing bioerosion rates of coral skeleton (Reyes-Nivia et al., 2013).

4.2 Future directions to sustain Hong Kong coral community health

Hong Kong coral communities live in a marginal environment of extremes and have been subject to a mix of anthropogenic and natural stressors that have contributed to their strong resilience and adaptability (Goodkin et al., 2011), while also reducing their structural complexity and, by extension, ecosystem function (Cybulski et al., 2020). This study demonstrates that these communities are net respiring across the east-west gradient. Therefore, Hong Kong corals may offer a glimpse into how coral communities may function, and how corals may adapt to marginal conditions expected to prevail more widely, in the future (Camp et al., 2018). Corals have already begun shifting their distributions poleward (Price et al., 2019) as the equatorial tropics pass thermal limits for coral survival (but see Huang et al.,2024, as this may be a cryptic species artefact rather than increased poleward migration). Additionally, as coastal areas become increasingly influenced by the effects of urbanization (Hugo, 2011), studying how sub-tropical, urbanized corals are persisting under already marginal conditions is a critical area of research (Schoepf et al., 2023). Certain environmental conditions unique to urbanized reefs such as enhanced near-shore turbidity have already been shown to help protect corals from light- and temperature-induced bleaching (Morgan et al., 2017; Sully & van Woesik, 2020) and overall heat stress (Cannon et al., 2023).

Measuring coral community metabolism in this type of environment can provide critical insights into what environmental drivers assist the overall community (not just corals) to persist even with negative budgets for both net production and net calcification, and how these drivers may change over space and time. This includes all metabolically active organisms contributing to enhanced biodiversity found in coral habitats, such as fishes, algae, and bioeroders like urchins and other bivalves. These have been reported as an overlooked but vital part of the community that can directly influence coral growth rates in Hong Kong (Yeung et al., 2021).

https://doi.org/10.5194/egusphere-2026-719
Preprint. Discussion started: 16 February 2026

By gathering empirical data on NEP rates at high temporal resolution over coral communities around Hong Kong, this study improves our understanding of what local conditions influence the degree of marginality that corals are subjected to within a larger highly urbanized marine ecosystem, such as hydrodynamics (Grimaldi et al., 2023), depth (Page et al., 2019; Cyronak et al., 2020), benthic composition (Page et al., 2017), or nutrient levels (Becker et al., 2021). The approach outlined can aid in determining which sites are best suited for future restoration efforts by highlighting what environments are conducive to continued calcification and production. This study suggests there may be limited options for optimal coral restoration sites around Hong Kong; even areas more removed from the Pearl River and anthropogenic pressures that maintain relatively high coral cover are net dissolving and net respiring. More studies looking at in-situ metabolism rates of corals across Hong Kong, perhaps in locations where restoration projects have already been carried out, such as Tolo Harbour (World Wildlife Fund, 2025), Bluff Island (ARCHIREEF, 2025) and Hoi Ha Wan (AFCD, 2019), would be beneficial in elucidating conducive environments for coral restoration in Hong Kong, where environmental conditions fluctuate widely over small local scales. Community metabolism was negative across the environmental gradient examined, reinforcing that these coral communities are likely to struggle to sustain positive growth within this marginal environment.

5 Conclusions

Even under marginal conditions, the environmental factors dictating community-scale metabolic rates vary markedly seasonally and in response to small-scale variations in local conditions. This study demonstrated such variability in metabolic signals over coral communities persisting under marginal environments around Hong Kong. NEP rates were negative or only slightly positive for all sites and each season, demonstrating overall suppressed productivity at a community scale. Wet season NEP was lower and more variable than the dry season at all three study sites. These suppressed NEP rates indicate that coral communities across Hong Kong have limited potential for growth or high functionality under prevailing environmental conditions.

More studies investigating metabolic patterns in corals subject to highly variable and marginal environmental conditions will increase the data available to model and predict future changes in coral ecosystem functioning in response to climate change and local stressors. Furthermore, such data and models can help to identify marine environments that are more suited for management efforts and restoration projects, or conversely unlikely to support functioning coral communities in the future. We advocate for more widespread collection of concurrent high-temporal-resolution, in-situ biophysical and metabolic data over coral communities across the globe to further our knowledge of community-level metabolism and ecosystem functioning under marginal conditions likely to dominate coastal habitats in the future.

.

https://doi.org/10.5194/egusphere-2026-719
Preprint. Discussion started: 16 February 2026

Data availability

Environmental water quality data around Hong Kong can be obtained from the Environmental Protection Department (EPD; https://cd.epic.epd.gov.hk/EPICRIVER/marine/?lang=en), while weather observations are provided by Hong Kong Observatory (HKO; https://www.hko.gov.hk). Environmental and community composition data collected during this study have been archived at PANGAEA (https://www.pangaea.de/).

Supplement link

Supplementary Information attached.

Author contributions

T.B.K.: Conceptualization (equal), Data curation (lead), Formal Analysis (lead) Investigation (lead), Methodology (lead), Project Administration (supporting), Validation (lead), Visualization (lead), Writing – Original Draft Preparation (lead), Writing – Review & Editing (lead). **Y-D.P.:** Formal Analysis (supporting), Investigation (supporting), Methodology (supporting), Project Administration (supporting), Writing – Review & Editing (supporting). **J.B-W.:** Investigation (supporting), Project Administration (supporting), Writing – Review & Editing (supporting). **A.S.J.W.:** Conceptualization (equal), Data curation (supporting), Funding Acquisition (lead), Investigation (supporting), Methodology (supporting), Project Administration (lead), Resources (lead), Supervision (lead), Writing – Original Draft Preparation (supporting), Writing – Review & Editing (supporting).

Competing interests

The authors have declared no competing interests.

Disclaimer

Copernicus Publications remains neutral with regard to jurisdictional claims made in the text, published maps, institutional affiliations, or any other geographical representation in this paper. While Copernicus Publications makes every effort to include appropriate place names, the final responsibility lies with the authors. Views expressed in the text are those of the authors and do not necessarily reflect the views of the publisher.

https://doi.org/10.5194/egusphere-2026-719
Preprint. Discussion started: 16 February 2026

Acknowledgements

Thank you to C. Skinner for assistance with early field seasons and to the skilled boat captains Wong, C.W., Kwok, V., and Tong V. for field work support. Field deployments were performed under permits '(47) in AF MPD 09/3 Pt.24', '(2) in AF MPD 09_3 Pt.25', and '(27) in AF MPD 09_3 Pt.25' from the Hong Kong Agriculture, Fisheries and Conservation Department (AFCD).

Financial support

The work was partially supported by funding from the Hong Kong Branch of the Southern Marine Science and Engineering Laboratory Guangdong Laboratory (Guangzhou) (SMSEGL20SC01) and Research Grants Council (RGC) of Hong Kong (RGC project number AoE/P-601/23-N). TK, YDP, and JBW were supported by the RGC Hong Kong PhD Fellowship Scheme (HKPFS PF19-35625, PF22-74876, and PF21-66378, respectively).

References

AFCD. *Hard coral restoration in Hoi Ha Wan Marine Park (Part 1).* Accessed 2024 August 2. Available from https://www.afcd.gov.hk/english/country/cou_vis/cou_vis_mar/cou_vis_mar_mon/files/HCR_e.pdf., 2019.

Albright, R., Langdon, C., & Anthony, K. R. N. Dynamics of seawater carbonate chemistry, production, and calcification of a coral reef flat, central Great Barrier Reef. *Biogeosciences*, *10*(10), 6747-6758. https://doi.org/10.5194/bg-10-6747-2013, 2013.

Andersson, A. J., & Gledhill, D. Ocean acidification and coral reefs: Effects on breakdown, dissolution, and net ecosystem calcification. *Annual Review of Marine Science*, *5*, 321–348. https://doi.org/10.1146/annurev-marine-121211-172241. 2013.

ARCHIREEF. (2025). *Sino Group Harbour of Love.* Accessed 2025 April 15. Available from https://archireef.co/sino-group/.

Barnes, D. J.. Profiling coral reef productivity and calcification using pH and oxygen electrodes. *Journal of Experimental Marine Biology and Ecology*, *66*(2), 149–161. https://doi.org/10.1016/0022-0981(83)90036-9. 2025

Becker, D. M., Putnam, H. M., Burkepile, D. E., Adam, T. C., Vega Thurber, R., & Silbiger, N. J. Chronic low-level nutrient enrichment benefits coral thermal performance in a fore reef habitat. *Coral Reefs*, *40*(5), 1637-1655. https://doi.org/10.1007/s00338-021-02138-2. 2021

Beijbom, O., Edmunds, P. J., Roelfsema, C., et al. Towards automated annotation of benthic survey images: Variability of human experts and operational modes of automation. *PloS one*, *10*(7), e0130312. https://doi.org/10.1371/journal.pone.0130312, 2015

Bellwood, D. R., Streit, R. P., Brandl, S. J., & Tebbett, S. B. The meaning of the term 'function' in ecology: A coral reef perspective. *Functional Ecology, 33*(6), 948-961. https://doi.org/10.1111/1365-2435.13265, 2019.

https://doi.org/10.5194/egusphere-2026-719
Preprint. Discussion started: 16 February 2026

Burt, J. A., Camp, E. F., Enochs, I. C., et al. Insights from extreme coral reefs in a changing world. In *Coral Reefs* (Vol. 39, Issue 3, pp. 495–507). https://doi.org/10.1007/s00338-020-01966-y, 2020

Camp, E. F., Schoepf, V., Mumby, P. J., Hardtke, L. A., Rodolfo-Metalpa, R., Smith, D. J., & Suggett, D. J. The future of coral reefs subject to rapid climate change: lessons from natural extreme environments. *Frontiers in Marine Science*, *5*, 4. https://doi.org/10.3389/fmars.2018.00004, 2018.

Cannon, S., Liu, A., & Donner, S. Interactions between local disturbance and climate-driven heat stress on central Pacific coral reefs. *Marine Ecology Progress Series*. https://doi.org/10.3354/meps14284. 2023

Cheung-Wong, R. W., Dytnerski, J. K., Gotama, R., Hemraj, D. A., & Russell, B. D. Seasonal patterns of macroalgal and sessile invertebrate communities in a monsoonal marine ecosystem. *Estuarine, Coastal and Shelf Science*, *275*, 107962. https://doi.org/10.1016/j.ecss.2022.107962, 2022.

Chung, S. S., Au, A., & Qiu, J. W. Understanding the underwater behaviour of scuba divers in Hong Kong. *Environmental management*, *51*, 824-837. https://doi.org/10.1007/s00267-013-0023-y, 2013

Chung, T. H., Dellisanti, W., Lai, K. P., Wu, J., Qiu, J. W., & Chan, L. L. Local conditions modulated the effects of marine heatwaves on coral bleaching in subtropical Hong Kong waters. *Coral Reefs*, *43*(5), 1235-1247. https://doi.org/10.1007/s00338-024-02533-5, 2024

Comeau, S., Edmunds, P. J., Spindel, N. B., & Carpenter, R. C. Fast coral reef calcifiers are more sensitive to ocean acidification in short-term laboratory incubations. *Limnology and Oceanography*, *59*(3), 1081-1091. https://doi.org/10.4319/lo.2014.59.3.1081, 2014

Coogan, J., Rheuban, J. E., & Long, M. H. Evaluating benthic flux measurements from a gradient flux system. *Limnology and Oceanography: Methods*. https://doi.org/10.1002/lom3.10482, 2022

Cryer, S. E., Evans, C., Fowell, S. E., Andrews, G., Brown, P., Carvalho, F., ... & Loucaides, S. Characterizing Reef Net Metabolism Via the Diel Co-Variation of pH and Dissolved Oxygen From High Resolution in Situ Sensors. *Global Biogeochemical Cycles*, *37*(9), e2022GB007577. https://doi.org/10.1029/2022GB007577, 2023

Cybulski, J. D., Husa, S. M., Duprey, N. N., et al. Coral reef diversity losses in China's Greater Bay Area were driven by regional stressors. In *Sci. Adv* (Vol. 6). DOI:10.1126/sciadv.abb1046, 2020.

Cyronak, T., Andersson, A. J., Langdon, C., et al. Taking the metabolic pulse of the world's coral reefs. *PloS one*, *13*(1). https://doi.org/10.1371/journal.pone.0190872, 2018

Cyronak, T., Takeshita, Y., Courtney, T. A., et al. Diel temperature and pH variability scale with depth across diverse coral reef habitats. *Limnology and Oceanography Letters*, *5*(2), 193-203. https://doi.org/10.1002/lol2.10129, 2020

DeCarlo, T. M., Cohen, A. L., Wong, G. T., et al. Community production modulates coral reef pH and the sensitivity of ecosystem calcification to ocean acidification. *Journal of Geophysical Research: Oceans*, *122*(1), 745-761. https://doi.org/10.1002/2016JC012326, 2017

https://doi.org/10.5194/egusphere-2026-719
Preprint. Discussion started: 16 February 2026

Dellisanti, W., Tsang, R. H. L., Ang, P., Wu, J., Wells, M. L., & Chan, L. L. A Diver-Portable Respirometry System for in-situ Short-Term Measurements of Coral Metabolic Health and Rates of Calcification. *Frontiers in Marine Science*, *7*(November), 1–19. https://doi.org/10.3389/fmars.2020.571451, 2020.

Dickson, A. G., Sabine, C. L., & Christian, J. R. *Guide to best practices for ocean CO2 measurements*. PICES Special Publication 3, 191 pp., 2007

Doney, S. C., Fabry, V. J., Feely, R. A., & Kleypas, J. A. Ocean acidification: The other CO2 problem. In *Annual Review of Marine Science* (Vol. 1, pp. 169–192). https://doi.org/10.1146/annurev.marine.010908.163834, 2009

Dumont, C. P., Lau, D. C. C., Astudillo, J. C., Fong, K. F., Chak, S. T. C., & Qiu, J. W. Coral bioerosion by the sea urchin Diadema setosum in Hong Kong: Susceptibility of different coral species. *Journal of Experimental Marine Biology and Ecology*, *441*, 71–79. https://doi.org/10.1016/j.jembe.2013.01.018, 2013

Duprey, N. N., Yasuhara, M., & Baker, D. M. Reefs of tomorrow: Eutrophication reduces coral biodiversity in an urbanized seascape. *Global Change Biology, 22*(11), 3550–3565. https://doi.org/10.1111/gcb.13302, 2016.

Duprey, N. N., McIlroy, S. E., Ng, T. P. T., et al. Facing a wicked problem with optimism: issues and priorities for coral conservation in Hong Kong. *Biodiversity and Conservation*, *26*(11), 2521-2545. https://doi.org/10.1007/s10531-017-1383-z, 2017.

Duprey, N. N., Wang, T. X., Kim, T., et al. Megacity development and the demise of coastal coral communities: Evidence from coral skeleton δ15N records in the Pearl River estuary. *Global Change Biology, 26*(3), 1338–1353. https://doi.org/10.1111/gcb.14923, 2020

Edmunds, P. J., Comeau, S., Lantz, C., et al. Integrating the effects of ocean acidification across functional scales on tropical coral reefs. *Bioscience*, *66*(5), 350-362. https://doi.org/10.1093/biosci/biw023, 2016

Fabricius, K. E., De'Ath, G., Puotinen, M. L., Done, T., Cooper, T. F., & Burgess, S. C. Disturbance gradients on inshore and offshore coral reefs caused by a severe tropical cyclone. *Limnology and Oceanography*, *53*(2), 690-704. https://doi.org/10.4319/lo.2008.53.2.0690, 2008.

Falter, J. L., Lowe, R. J., Atkinson, M. J., & Cuet, P. Seasonal coupling and de-coupling of net calcification rates from coral reef metabolism and carbonate chemistry at Ningaloo Reef, Western Australia. *Journal of Geophysical Research: Oceans*, *117*(C5). https://doi.org/10.1029/2011JC007268, 2012.

Goodkin, N. F., Switzer, A. D., McCorry, D., et al. Coral communities of Hong Kong: Long-lived corals in a marginal reef environment. *Marine Ecology Progress Series*, *426*(August 2015), 185–196. https://doi.org/10.3354/meps09019, 2011.

Grimaldi, C. M., Lowe, R. J., Benthuysen, J. A., Cuttler, M. V. W., Green, R. H., & Gilmour, J. P. Hydrodynamic and atmospheric drivers create distinct thermal environments within a coral reef atoll. *Coral Reefs*, *42*(3), 693-706. https://doi.org/10.1007/s00338-023-02371-x, 2023.

Gross, T. F., & Nowell, A. R. Mean flow and turbulence scaling in a tidal boundary layer. *Continental Shelf Research*, *2*(2-3), 109-126. https://doi.org/10.1016/0278-4343(83)90011-0, 1983

https://doi.org/10.5194/egusphere-2026-719
Preprint. Discussion started: 16 February 2026

672 Harmelin-Vivien, M. L. The effects of storms and cyclones on coral reefs: a review. *Journal of Coastal Research*, 211-231.
673 http://www.jstor.org/stable/25735600, 1994.
674 Haas, A. F., Fairoz, M. F., Kelly, L. W., Nelson, C. E., Dinsdale, E. A., Edwards, R. A., ... & Rohwer, F. Global
675 microbialization of coral reefs. *Nature microbiology*, *1*(6), 1-7. https://doi.org/10.1038/nmicrobiol.2016.42, 2016.
676 Heery, E. C., Hoeksema, B. W., Browne, N. K., et al. Urban coral reefs: Degradation and resilience of hard coral assemblages
677 in coastal cities of East and Southeast Asia. *Marine Pollution Bulletin*, *135*, 654–681.
678 https://doi.org/10.1016/j.marpolbul.2018.07.041, 2018.
679 Hong Kong Observatory. *Solar energy resources in Hong Kong from a climatological point of view*. Accessed 2024 December
680 21. Available from: https://www.hko.gov.hk/en/education/weather/sunshine-and-uv/00443-solar-energy-resources-in-
681 hong-kong-from-a-climatological-point-of-view.html, 2022.
682 Hong Kong Observatory. *Hourly meteorological data for Hong Kong, including rainfall, temperature, wind, and solar*
683 *radiation (2013–2022)*. Accessed 2024 September 09. Available from: https://www.hko.gov.hk, 2025.
684 Huang, Y. Y., Chen, T. R., Lai, K. P., et al. Poleward migration of tropical corals inhibited by future trends of seawater
685 temperature and calcium carbonate ($CaCO_3$) saturation. *The Science of the Total Environment, 929*, 172562.
686 https://doi.org/10.1016/j.scitotenv.2024.172562, 2024.
687 Hughes, T. P., Kerry, J. T., Álvarez-Noriega, M., et al. Global warming and recurrent mass bleaching of
688 corals. *Nature*, *543*(7645), 373-377. https://doi.org/10.1038/nature21707, 2017.
689 Hugo, G. Future demographic change and its interactions with migration and climate change. *Global Environmental Change*,
690 *21*(SUPPL. 1). https://doi.org/10.1016/j.gloenvcha.2011.09.008, 2011.
691 Jackson, J. B. C., Kirby, M. X., Berger, W. H., et al. *Historical Overfishing and the Recent Collapse of Coastal Ecosystems*.
692 DOI:10.1126/science.1059199, 2001
693 Kekuewa, S. A. H., Courtney, T. A., Cyronak, T., et al. Temporal and Spatial Variabilities of Chemical and Physical
694 Parameters on the Heron Island Coral Reef Platform. *Aquatic Geochemistry*. https://doi.org/10.1007/s10498-021-
695 09400-7, 2021.
696 Khrizman, A., Lindhart, M., Mucciarone, D. A., Takeshita, Y., Monismith, S. G., Boles, E. L., & Dunbar, R. B. Reef
697 Community Productivity and Calcification–Spatial and Temporal Variability in Recovering Coral Reefs. *Journal of*
698 *Geophysical Research: Oceans*, *130*(3), e2024JC021592. https://doi.org/10.1029/2024JC021592, 2025.
699 Kinsey, D. W. Metabolism, calcification and carbon production: I. System level studies. *Proceedings of the 5th International*
700 *Coral Reef Congress, Tahiti, 27 May–1 June 1985*, 4, 503–542. 11068/3465, 1985.
701 Lau, S. C., Thomas, M., Hancock, B., & Russell, B. D. Restoration potential of Asian oysters on heavily developed
702 coastlines. *Restoration Ecology*, *28*(6), 1643-1653. https://doi.org/10.1111/rec.13267, 2020.
703 Law, M. T., & Huang, D. Light limitation and coral mortality in urbanised reef communities due to sea-level rise. *Climate*
704 *Change Ecology*, *5*, 100073. https://doi.org/10.1016/j.ecochg.2023.100073, 2023.

https://doi.org/10.5194/egusphere-2026-719
Preprint. Discussion started: 16 February 2026

Lombardi, M. R., Lesser, M. P., & Gorbunov, M. Y. Fast repetition rate (FRR) fluorometry: variability of chlorophyll a fluorescence yields in colonies of the corals, Montastraea faveolata (w.) and Diploria labyrinthiformes (h.) recovering from bleaching. *Journal of experimental marine biology and ecology*, *252*(1), 75-84. https://doi.org/10.1016/S0022-0981(00)00238-0, 2000.

Lowe, A. T., Bos, J., & Ruesink, J. Ecosystem metabolism drives pH variability and modulates long-term ocean acidification in the Northeast Pacific coastal ocean. *Scientific Reports*, *9*(1), 963. https://doi.org/10.1038/s41598-018-37764-4, 2019.

Mallon, J., Cyronak, T., Hall, E. R., Banaszak, A. T., Exton, D. A., & Bass, A. M. Light-driven dynamics between calcification and production in functionally diverse coral reef calcifiers. *Limnology and Oceanography*, *67*(2), 434-449. https://doi.org/10.1002/lno.12002, 2022.

McGillis, W. R., Langdon, C., Loose, B., Yates, K. K., & Corredor, J. Productivity of a coral reef using boundary layer and enclosure methods. *Geophysical Research Letters*, *38*(3), 2–6. https://doi.org/10.1029/2010GL046179, 2011.

McIlroy, S. E., Thompson, P. D., Yuan, F. L., Bonebrake, T. C., & Baker, D. M. Subtropical thermal variation supports persistence of corals but limits productivity of coral reefs. *Proceedings of the Royal Society B*, *286*(1907), 20190882. https://doi.org/10.1098/rspb.2019.0882, 2019.

McIlroy, S. E., Guibert, I., Archana, A., et al. Life goes on: Spatial heterogeneity promotes biodiversity in an urbanized coastal marine ecosystem. *Global Change Biology*, *30*(4), e17248. https://doi.org/10.1111/gcb.17248, 2024.

Meléndez, M., Salisbury, J., Gledhill, D., et al. Net ecosystem dissolution and respiration dominate metabolic rates at two western Atlantic reef sites. *Limnology and Oceanography, 67*, 527–539. https://doi.org/10.1002/lno.12009, 2022.

Millero, F. J. Thermodynamics of the carbon dioxide system in the oceans. In *Geochimica et Cosmochimica Acta* (Vol. 59, Issue 4). https://doi.org/10.1016/0016-7037(94)00354-O, 1995.

Moberg, F., & Folke, C. Ecological goods and services of coral reef ecosystems. *Ecological Economics*, *29*(2), 215–233. https://doi.org/10.1016/S0921-8009(99)00009-9, 1999.

Morgan, K. M., Perry, C. T., Johnson, J. A., & Smithers, S. G. Nearshore turbid-zone corals exhibit high bleaching tolerance on the Great Barrier Reef following the 2016 ocean warming event. *Frontiers in Marine Science*, *4*(JUL). https://doi.org/10.3389/fmars.2017.00224, 2017.

Morton, B. Pollution of the coastal waters of Hong Kong. *Marine Pollution Bulletin*, *20*(7), 310-318. https://doi.org/10.1016/0025-326X(89)90153-7, 1989.

NASA Langley Research Center (LaRC), POWER Project. *Surface meteorology and solar energy data for the Caribbean region (NASA SSE v4.0)*. Accessed 2024 June 01. Available from: https://power.larc.nasa.gov, 2025.

Page, H. N., Courtney, T. A., Collins, A., De Carlo, E. H., & Andersson, A. J. Net community metabolism and seawater carbonate chemistry scale non-intuitively with coral cover. *Frontiers in Marine Science*, *4*, 161. https://doi.org/10.3389/fmars.2017.00161, 2017.

https://doi.org/10.5194/egusphere-2026-719
Preprint. Discussion started: 16 February 2026

Page, H. N., Courtney, T. A., De Carlo, E. H., Howins, N. M., Koester, I., & Andersson, A. J. Spatiotemporal variability in seawater carbon chemistry for a coral reef flat in Kāne ʻohe Bay, Hawai ʻi. *Limnology and Oceanography*, *64*(3), 913-934. https://doi.org/10.1002/lno.11084, 2019.

Pezner, A. K., Courtney, T. A., Barkley, H. C., Chou, W. C., Chu, H. C., Clements, S. M., ... & Andersson, A. J. Increasing hypoxia on global coral reefs under ocean warming. *Nature Climate Change*, *13*(4), 403-409. https://doi.org/10.1038/s41558-023-01619-2, 2023.

Platz, M. C., Takeshita, Y., Bartels, E., & Arias, M. E. Evaluating the potential for autonomous measurements of net community production and calcification as a tool for monitoring coral restoration. *Ecological Engineering*, *158*(August), 106042. https://doi.org/10.1016/j.ecoleng.2020.106042, 2020.

Platz, M. C., Arias, M. E., & Byrne, R. H. Reef metabolism monitoring methods and potential applications for coral restoration. *Environmental Management*, *69*(3), 612-625. https://doi.org/10.1007/s00267-022-01597-9, 2022.

Price, N. N., Muko, S., Legendre, L., et al. Global biogeography of coral recruitment: Tropical decline and subtropical increase. *Marine Ecology Progress Series*, *621*, 1–17. https://doi.org/10.3354/meps12980, 2019.

Reyes-Nivia, C., Diaz-Pulido, G., Kline, D., Guldberg, O. H., & Dove, S. Ocean acidification and warming scenarios increase microbioerosion of coral skeletons. *Global change biology*, *19*(6), 1919-1929. https://doi.org/10.1111/gcb.12158, 2013.

Schneider, K., Silverman, J., Woolsey, E., Eriksson, H., Byrne, M., & Caldeira, K. Potential influence of sea cucumbers on coral reef CaCO3 budget: A case study at One Tree Reef. *Journal of Geophysical Research: Biogeosciences*, *116*(G4)., https://doi.org/10.1029/2011JG001755, 2011.

Schoepf, V., Cornwall, C.E., Pfeifer, S.M. et al. Impacts of coral bleaching on pH and oxygen gradients across the coral concentration boundary layer: a microsensor study. *Coral Reefs* **37**, 1169–1180. https://doi.org/10.1007/s00338-018-1726-6, 2018.

Schoepf, V., Baumann, J. H., Barshis, D. J., et al. Corals at the edge of environmental limits: A new conceptual framework to re-define marginal and extreme coral communities. *Science of The Total Environment*, *884*, 163688. https://doi.org/10.1016/j.scitotenv.2023.163688, 2023.

SolarGIS s.r.o. *Solar radiation data for the Red Sea (01 Jan 2013–31 Dec 2022)*. Accessed 2024 June 1. Available from: https://solargis.com, 2025

Solcast Pty Ltd. *Solar irradiance data for the Great Barrier Reef (01 Jan 2013–31 Dec 2022)*. Accessed 2024 June 1. Available from: https://solcast.com, 2025.

Stoltenberg, L., Schulz, K. G., Cyronak, T., & Eyre, B. D. Seasonal variability of calcium carbonate precipitation and dissolution in shallow coral reef sediments. *Limnology and Oceanography*, *65*(4), 876–891. https://doi.org/10.1002/lno.11357, 2020.

Sully, S., & van Woesik, R. Turbid reefs moderate coral bleaching under climate-related temperature stress. *Global Change Biology*, *26*(3), 1367–1373. https://doi.org/10.1111/gcb.14948, 2020.

https://doi.org/10.5194/egusphere-2026-719
Preprint. Discussion started: 16 February 2026

Takeshita, Y., Mcgillis, W., Briggs, E. et al. Journal of Geophysical Research: Oceans coral reef using a boundary layer approach. *Journal of Geophysical Research: Oceans*, 5655–5671. https://doi.org/10.1002/2016JC011886, 2016.

Takeshita, Y., Cyronak, T., Martz, T. R., Kindeberg, T., & Andersson, A. J. Coral reef carbonate chemistry variability at different functional scales. *Frontiers in Marine Science*, *5*(MAY). https://doi.org/10.3389/fmars.2018.00175, 2018.

Thomas, L., Rose, N. H., Bay, R. A., et al. Mechanisms of thermal tolerance in reef-building corals across a fine-grained environmental mosaic: lessons from Ofu, American Samoa. *Frontiers in Marine Science*, *4*, 434. https://doi.org/10.3389/fmars.2017.00434, 2018.

Travaglione, N., Evans, R., Moustaka, M., et al. Scleractinian corals rely on heterotrophy in highly turbid environments. *Coral Reefs*, *42*(5), 997-1010. https://doi.org/10.1007/s00338-023-02407-2, 2023.

Turk, D., Yates, K. K., Vega-Rodriguez, M., et al. Community metabolism in shallow coral reef and seagrass ecosystems, lower Florida Keys. *Marine Ecology Progress Series*, *538*, 35–52. https://doi.org/10.3354/meps11385, 2015.

Tuttle, L. J., & Donahue, M. J. Effects of sediment exposure on corals: a systematic review of experimental studies. *Environmental Evidence*, *11*(1), 4. https://doi.org/10.1186/s13750-022-00256-0, 2022.

Uppstrom, L. R. *The boron/chlorinity ratio of deep-sea water from the Pacific Ocean* (Vol. 21). Pergamon Press. https://doi.org/10.1016/0011-7471(74)90074-6, 1974.

Wang, W., Cai, S., Huang, J., Ding, R., & Chen, L. Variation in the Quanta-to-Energy Ratio of Photosynthetically Active Radiation under the Cloudless Atmosphere. *Atmosphere*, *15*(10), 1166. https://doi.org/10.3390/atmos15101166, 2024.

World Wildlife Fund. *Reviving our corals Reviving corals, reviving our oceans.* Accessed 2025 April 17. Available from https://revivingourcorals.wwf.org.hk/, 2025

Xie, J. Y., Yeung, Y. H., Kwok, C. K., et al. Localized bleaching and quick recovery in Hong Kong's coral communities. *Marine Pollution Bulletin*, *153*, 110950. https://doi.org/10.1016/j.marpolbul.2020.110950, 2020.

Yeung, Y. H., Xie, J. Y., Zhao, Y., et al. Rapid external erosion of coral substrate in subtropical Hong Kong waters. *Marine Pollution Bulletin*, *169*. https://doi.org/10.1016/j.marpolbul.2021.112495, 2021.

Zhao, Y., Chen, M., Chung, T. H., Chan, L. L., & Qiu, J. W. The 2022 summer marine heatwaves and coral bleaching in China's Greater Bay Area. *Marine Environmental Research, 189*, 106044. https://doi.org/10.1016/j.marenvres.2023.106044, 2023.

Zhou, W., Yin, K., Harrison, P. J., & Lee, J. H. W. The influence of late summer typhoons and high river discharge on water quality in Hong Kong waters. *Estuarine, Coastal and Shelf Science, 111*, 35–47. https://doi.org/10.1016/j.ecss.2012.06.004, 2012.